A simple, versatile approach for coupling a liquid chromatograph and chemical ionization mass spectrometer for offline analysis of organic aerosol

Andre F. Schaum^{1,2}, Kelvin H. Bates³, Kyung-Eun Min^{2,4}, Faith Myers², Emmaline R. Longnecker^{1,2}, Manjula R. Canagaratna⁵, Mitchell W. Alton⁵, Paul J. Ziemann^{1,2}

Correspondence to: P. J. Ziemann (pazi4520@colorado.edu)

Abstract.

A method is described for coupling a high-performance liquid chromatograph (HPLC) and chemical ionization mass spectrometer (CIMS) for offline analysis of organic aerosol. It employs a nebulizer interface and a Vaporization Inlet for Aerosols (VIA), allowing for the transmission of analytes from the HPLC eluent into the CIMS inlet. Performance of the HPLC-VIA-CIMS system was assessed through analysis of carboxylic acid standards, environmental chamber-generated secondary organic aerosol (SOA) formed from the ozonolysis of α-pinene, and ambient OA collected at an urban setting. Chromatographic peak shapes were retained through nebulization and evaporation, providing baseline-resolved separation of C₆-C₁₈ carboxylic acids and generating molecular-level detail that is not attainable using HPLC or CIMS alone. Instrument response was found to be linear (R²>0.97) over an order of magnitude (0.2–3.0 nmol or 2–30 nmol on column) for each of the 12 standards. Analysis of α-pinene ozonolysis SOA achieved isomer-resolved detection of both monomer and dimer reaction products and, through the use of a diode array detector (DAD), illustrated the preservation of chromatographic peak shape through nebulization and evaporation. The HPLC-VIA-CIMS instrument also shows potential for quantitative analysis, provided that authentic standards can be purchased or synthesized, and semiquantitative analysis of UV-absorbing compounds such as nitrates and carboxylic acids by using a DAD. The system is compatible with small sample quantities (e.g., 30 μg of α-pinene ozonolysis SOA), allowing for detailed molecular characterization of field-collected SOA, including the identification of several monoterpene oxidation products.

1 Introduction

Atmospheric aerosols, particularly those smaller than 1 µm in diameter, present direct risks to human health and can influence global climate through their contributions to radiative forcing (Pöschl, 2005). These effects are highly dependent on the

¹Department of Chemistry, University of Colorado, Boulder, Colorado 80309, United States

²Cooperative Institute for Research in Environmental Sciences (CIRES), Boulder, Colorado 80309, United States

³Department of Mechanical Engineering, University of Colorado Boulder, Boulder, Colorado 80309, United States

⁴School of Environment and Energy Engineering, Gwangju Institute of Science and Technology, 61005, Gwangju, South Korea

⁵Aerodyne Research Inc., Billerica, Massachusetts 01821, United States

chemical and physical properties of aerosol particles (Mauderly and Chow, 2008; Shrivastava et al., 2017), highlighting the need for analytical techniques that can provide detailed information about their composition. Characterization of organic aerosol at a molecular level, however, is challenging due to the chemical complexity (>10⁴ known compounds) produced by the oxidation of volatile organic compounds (VOCs) to low-volatility products that form secondary organic aerosol (SOA) (Goldstein and Galbally, 2007). The constituents of SOA are often multifunctional, containing combinations of nitrate, hydroxyl, carboxyl, carbonyl, peroxide, and other oxygen-containing functional groups that influence the physicochemical properties of the aerosols (Kroll and Seinfeld, 2008; Ziemann and Atkinson, 2012).

40

65

Real-time analysis of organic aerosol (OA) composition has most often been conducted using the Aerodyne Aerosol Mass Spectrometer (AMS) (Canagaratna et al., 2007), in which particles are sampled into a high-vacuum chamber, vaporized by impaction on a hot surface, and the vapor is analyzed by electron ionization mass spectrometry (EIMS). Compared to chemical ionization mass spectrometry (CIMS), the AMS has the advantage that it can be used to quantify the major OA components (e.g., oxidized, hydrocarbon-like, and biomass-burning OA) through the use of appropriate calibration and data analysis methods. It's disadvantage is that EI (combined with the 600 °C vaporization temperature) leads to extensive fragmentation that usually prevents assignment of compound molecular formulas. The fragmentation problem can usually be overcome by the use of CIMS, with the trade-off being the loss of OA quantitation except for single compounds when authentic molecular standards are available. In this case, particles are thermally desorbed before entering the CIMS ion-molecule reaction region, usually by passing through a heated tube at significantly lower temperatures than those used in the AMS. This approach has been employed with a large variety of CIMS reagent ions, for example: H⁺(H₂O)_n (Warscheid and Hoffmann, 2001); H⁺(H₂O)₂, H⁺(CH₃OH)₂, NO⁺, O₂⁺, O₂⁻, F⁻, SF₆⁻ (Hearn and Smith, 2004); H⁺(H₂O)_n, I⁻(H₂O)_n, CH₃C(O)O⁻ (Aljawhary et al., 2013); H₃O⁺ (Eichler et al., 2015); and NO₃⁻ (Häkkinen et al., 2023); which provide a wide range of ionization specificity and sensitivity that can be an advantage or disadvantage depending on the compounds of interest. Though effective at analyzing real-time changes in aerosol composition, these approaches usually fail to differentiate between isobaric species that commonly exist in SOA. One way to address this limitation is by coupling online ion mobility spectrometry with mass spectrometry (IMS-MS) (Krechmer et al., 2016), but use of this approach for atmospheric chemistry studies is in its infancy because until recently technical challenges have hindered the development of a commercial instrument with a reliable gas-phase ion source. Instead, methods employed to couple separation with MS have all involved semi-online or offline analysis.

The simplest of these has employed sample preconcentration and programmed thermal desorption for semi-online analysis, as with the thermal desorption particle beam mass spectrometer (TDPBMS) (Tobias and Ziemann, 1999), thermal desorption chemical ionization mass spectrometer (TDCIMS) (Voisin et al., 2003), and Filter Inlet for Gases and Aerosols (FIGAERO) (Cai et al., 2023). However, the resolution achieved by these methods is typically poor compared to other separation methods such as chromatography.

Gas chromatographic (GC) separation has been used in combination with CIMS instruments to resolve isomers and other closely related compounds in the atmosphere. Previous work includes analysis of VOCs by proton-transfer-reaction mass spectrometry (PTR-MS) (Warneke et al., 2003) and by I⁻ (Robinson et al., 2024) and CF₃O⁻ (Vasquez et al., 2018) CIMS as

well as aerosol by coupling a thermal desorption aerosol gas chromatograph (TAG) with I⁻ CIMS (Bi et al., 2021a, b). A disadvantage of using GC to separate OA constituents is the low transmission of multifunctional compounds through the column due to irreversible adsorption and/or thermal decomposition, although this can be ameliorated to some degree by chemical derivatization of hydroxyl, carbonyl, carboxyl (Yu et al., 1998, 1999), and hydroperoxide (Docherty et al., 2004) groups to increase analyte stability and volatility; and by the use of specialized GCs that utilize reduced pressure (Vasquez et al., 2018) or cryo-trapping (Robinson et al., 2024).

An alternative for compounds that are not amenable to the high temperatures used in GC analysis is high-performance liquid chromatography (HPLC), which is generally conducted at ambient temperature and offers flexibility in the choice of mobile phase and gradient elution for optimizing separations. HPLC has previously been used for analysis of SOA generated in environmental chambers and ambient SOA by coupling with several types of ionization and MS detection methods (Hildmann and Hoffmann, 2024). Electrospray ionization (ESI) is most commonly used (Hildmann and Hoffmann, 2024), though extractive electrospray ionization (EESI) (Schueneman et al., 2024), atmospheric pressure chemical ionization (APCI) (Hoffmann et al., 1998; Reinnig et al., 2008), atmospheric pressure photoionization (APPI) (Ruiz-Jiménez et al., 2012), and EI (Yeh and Ziemann, 2014) have also been employed. However, while these approaches are capable of separating complex mixtures and generating high-resolution mass spectra, the devices used to nebulize, vaporize, and ionize OA components following HPLC fractionation can suffer from matrix effects in ESI and EESI, and they are generally integrated in such a way as to allow limited opportunity for independently and easily varying the ionization method. This is a considerable drawback, considering the wide variety of CIMS reagent ions now available for selectively ionizing different compound classes and achieving exceptionally high detection sensitivity, the recently developed capability for rapidly switching among multiple reagent ions (Alton et al., 2024) for more comprehensive CIMS analysis, and the advantage of being able to analyze gas- and particle-phase compounds with the same CIMS methods.

Here, we describe a simple, versatile approach for coupling a HPLC to an I CIMS (I-CIMS) using a commercially available nebulizer and Aerodyne Vaporization Inlet for Aerosols (VIA) (Zhao et al., 2024) for the separation and analysis of SOA. The performance of the HPLC-VIA-CIMS system is first evaluated using a mixture of simple and functionalized carboxylic acid standards, and then through analysis of environmental chamber-generated SOA and an aerosol sample collected from an urban environment. Lastly, further applications and possible improvements to the system are discussed.

2 Materials and Methods

2.1 Chemicals

85

95

The following chemicals were used throughout the experiments described below: methanol (HPLC-grade, Fisher Chemical), acetonitrile (HPLC-grade, Fisher Chemical), Milli-Q water (18.2 MΩ, <5 ppb TOC), N₂ (ultrahigh purity, Airgas), glacial acetic acid (ACS-grade, Fisher Chemical), (1R)-(+)-α-pinene (99%, Sigma Aldrich), *cis*-pinonic acid (98%, Aldrich), *trans*-norpinic acid (Sigma Aldrich). Ozone was generated using a calibrated Ozone Engineering LG-7 ozone generator and pure O₂

(industrial-grade, Airgas). The organic acid standards had purities of at least >97% and included: adipic acid, suberic acid, sebacic acid, dodecanedioic acid, palmitic acid, stearic acid, and 16-hydroxypalmitic acid from TCI America; pimelic acid, azelaic acid, and 12-hydroxystearic acid from Thermo Scientific; undecanedioic acid and 2-hydroxypalmitic acid from MedChemExpress and Ambeed, Inc., respectively.

2.2 Environmental Chamber Experiment

100

105

110

Ozonolysis of α -pinene without the use of an OH scavenger was carried out in a 6.7 m³ Teflon chamber at ambient pressure (630 Torr) and temperature (22 °C) filled with dry air (<1% RH, <5 ppbv hydrocarbons) from two AADCO clean air generators. Approximately 500 ppb of ozone was added to the chamber using a calibrated glass bulb and the concentration was verified using a 2B Technologies Model 202 ozone monitor. Immediately following the ozone addition, 300 ppb of α -pinene was added using a custom-built vaporizer (Finewax et al., 2020). A Teflon-coated fan was used throughout each addition to mix the chamber air. The reaction was allowed to proceed for 40 min before sampling the SOA onto two preweighed Millipore Fluoropore PTFE filters (0.45 μ m pore size) at a flow rate of 14.2 LPM each for 1 h. After sampling, the filters were weighed, extracted twice with 6 mL acetonitrile, and evaporated under dry N₂ and stored at -10 °C until analysis. Extraction efficiency was determined to be ~98% based on the measured filter mass difference pre- and post-extraction. Prior to analysis, the SOA was reconstituted in methanol to achieve a total mass concentration of 2 mg mL⁻¹.

2.3 Field-Collected OA

Ambient OA was collected in October 2024 at the Denver, Colorado ASCENT site located approximately 4 km from downtown Denver in a suburban setting that also contains commercial activities (La Casa | ASCENT, 2024). Air quality at this site is influenced by anthropogenic and biogenic sources, including oil and gas operations and biomass burning. The OA sample was collected using an MCV high volume sampler (model CAV-A/mb) affixed with a PM1 sampling head operated at a flow rate of 30 m³ h⁻¹. The sampler collected aerosol onto a single Pall Tissuequartz filter (P.N. 7204) between the hours of 04:00 and 10:00 over the course of one week for a total of 42 h. At the end of the sampling period, the filters were transported on ice and stored at –10 °C until extraction. A full description of the extraction method and additional sampling details can be found in the Supplement.

2.4 Instrumentation

2.4.1 High Performance Liquid Chromatography

Analyses were performed using a Shimadzu Prominence HPLC system with a Nexera X2 SPD-M20A diode array detector (DAD) and an Agilent XBD-C8 column (150 x 4.6 mm, 5 µm). The aqueous mobile phase (A) consisted of 95% water, 5% acetonitrile, and 0.05% glacial acetic acid (v/v) whereas the organic mobile phase (B) was 95% methanol, 5% acetonitrile, and 0.05% glacial acetic acid (v/v). The addition of acetonitrile to the mobile phases serves as a dopant to suppress formation of

I·(H₂O)⁻ clusters and reduce the humidity dependence of the I-CIMS performance (Riva et al., 2024). Due to the large amount of water present in the HPLC eluent, omitting this addition results in significant depletion of the reagent ion and reduces instrument sensitivity. Although a mobile phase concentration of 5% was determined to be sufficient for the analyses described in this study, further optimization could be done to maximize instrument performance.

Mobile phase additives are commonly used in reverse-phase HPLC to modify eluent pH and improve peak shape and retention of ionizable analytes (e.g., carboxylic acids) (Schwarzenbach, 1982). However, analyte detection issues arise with typical pH modifiers such as formic acid and trifluoroacetic acid due to the relatively high sensitivity of I-CIMS to these acids. Acetic acid has been reported to have an I-CIMS sensitivity that is 30 times lower than that of formic acid (Lee et al., 2014) and was thus chosen as a pH modifier to improve the chromatography while limiting reagent ion depletion. Although the addition of a weak acid primarily served to improve the peak shapes of carboxylic acids in this study, it has been shown that lowering mobile phase pH can also improve the retention and peak shapes of basic analytes through ion pairing effects (Lobrutto et al., 2001). It is also worth noting that because compound evaporation and ionization are spatially separated in I-CIMS instruments (unlike in ESI), I-CIMS is not susceptible to ionization suppression caused by non-ideal electrospray conditions required to counteract the high conductivity and surface tension imparted to droplets by the organic acids (Apffel et al. (1995).

Gradient elution methods were used for analyte separation at a flow rate of 1 mL min⁻¹. The gradients used for the carboxylic acid standards, α-pinene SOA, and field-collected OA, respectively, were as follows: 20% B for 1.5 min, increase to 100% B over 12.5 min and hold for 5.5 min, return to initial conditions; 10% B for 1.5 min, increase to 80% B over 18 min, increase to 100% B over 0.5 min and hold for 3 min, return to initial conditions; 5% B for 1.5 min, increase to 100% B over 17.5 min and hold for 5 min, return to initial conditions. The HPLC-DAD chromatograms were baseline corrected using injections of solvent blanks.

2.4.2 VIA-CIMS

130

135

140

145

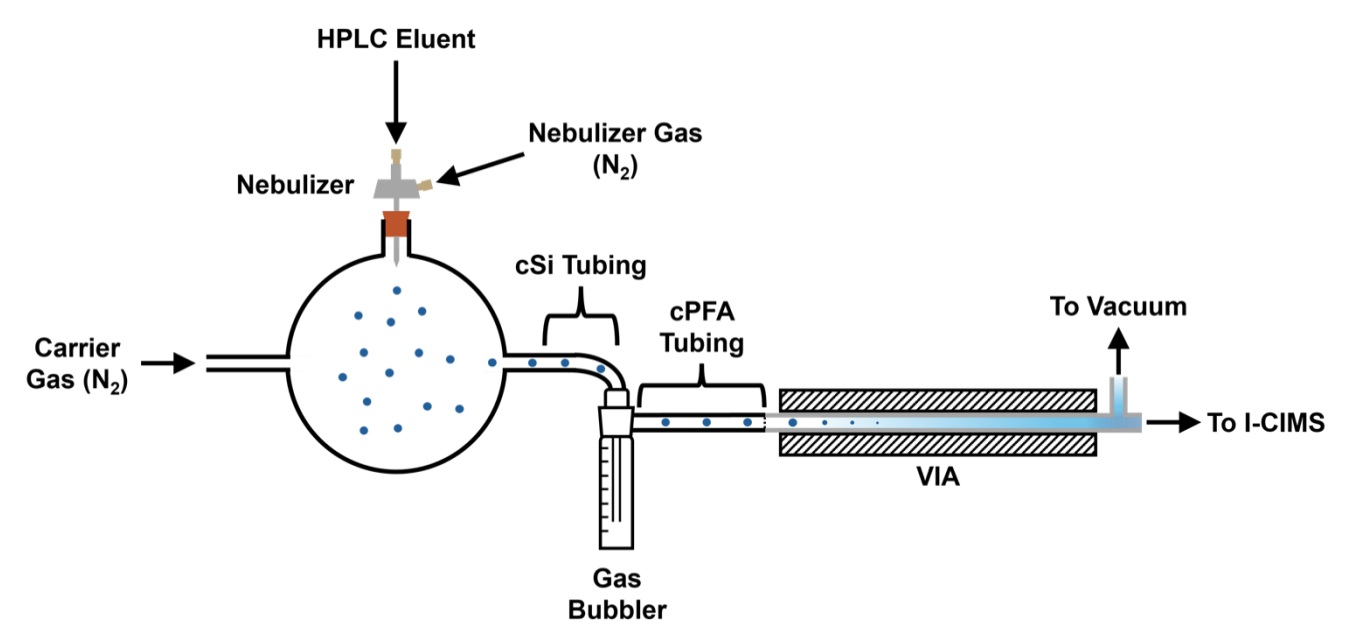
150 The I-CIMS instrument used for SOA analysis was previously described by DeVault et al. (2022a). Briefly, a Tofwerk ion mobility spectrometry-time-of-flight (IMS-TOF) mass spectrometer (Krechmer et al., 2016) with the IMS cell replaced by an iodide chemical ionization source was mounted with a VIA without the honeycomb activated carbon denuder to minimize analyte loss (Zhao et al., 2024). An additional vacuum line connected to a needle valve was installed immediately downstream of the VIA to increase the flow rate through the system above the I-CIMS inlet flow of 2 LPM. For all experiments the VIA was operated at a temperature of 200 °C and flow rate of 3.5 LPM to limit wall losses and thermal decomposition by reducing analyte residence time (Zhao et al., 2024). The I-CIMS data was processed using Tofware version 4.0.1 and chromatographic peak fitting was performed using the Multipeak Fitting package in IGOR Pro 9 (WaveMetrics).

2.4.3 Nebulizer Interface

160

165

The HPLC and I-CIMS inlet were coupled using a home-built nebulizer interface consisting of an electrospray nebulizer (Agilent EN10501) that was mounted in a three-port 300 mL glass bulb with a rubber stopper (Fig. 1). This bulb volume was chosen to maximize the distance between the nebulizer tip and the bottom of the bulb in order to reduce impaction of the nebulizer spray while not affecting peak broadening, as shown below. The nebulizer was supplied with N₂ at a pressure of 25 psi, resulting in a N₂ flow of 1.5 LPM, and the HPLC eluent was introduced at a flow rate of 1 mL min⁻¹. The total flow through the nebulizer bulb was adjusted to 3.5 LPM by flowing dry N₂ through a port orthogonal to the nebulizer spray; the N₂ flow rate was chosen to be consistent with the manufacturer's recommendations for VIA performance and was also found to optimize analyte signal in preliminary testing (Fig. S2). To prevent large droplets from reaching the VIA, a trap consisting of a 30 mL gas bubbler (Chemglass, CG-1821-01) with the glass frit removed was connected to the outlet of the glass bulb using 8 cm of conductive silicone tubing (4.5 mm ID, 9 mm OD). The gas bubbler outlet was connected to the VIA with 1 m of conductive PFA (cPFA) tubing (3/16" ID x 1/4" OD, Fluorotherm F015202G).



170 Figure 1: Schematic of nebulizer interface and VIA. HPLC eluent flowing at 1 mL min⁻¹ is nebulized into a glass bulb and the resulting solvent/analyte droplets are carried to the VIA by a total N₂ flow of 3.5 LPM. A gas bubbler (glass frit removed) prevents large droplets from reaching the VIA. The remaining droplets are vaporized in the VIA and proceed into the I-CIMS.

3. Results and Discussion

3.1 Separation and Detection of Carboxylic Acids

175 Since simple and functionalized organic acids are often found in SOA and have high I-CIMS sensitivities (Lee et al., 2014), a

selection of monocarboxylic acids, dicarboxylic acids, and hydroxycarboxylic acids were chosen as model analytes to evaluate the HPLC-VIA-CIMS performance. The organic acid standards (Table 1) were prepared in a solution of methanol at concentrations of 0.1 mM for the dicarboxylic acids and hydroxycarboxylic acids and 1 mM for palmitic acid and stearic acid. Figure 2 shows an HPLC-VIA-CIMS chromatogram of a 15 µL injection (1.5–15 nmol) of the standards separated over 18 min. In general, retention time is inversely correlated with analyte polarity for reverse-phase HPLC separations, meaning that more highly functionalized compounds will elute earlier than those with fewer functional groups. This is clearly observed in Fig. 2 with the dicarboxylic acids eluting first, followed by the hydroxycarboxylic acids and the monocarboxylic acids. It is important to note the baseline-resolved separation of 16- and 2-hydroxypalmitic acid, which are indistinguishable by molecular formula alone and are unlikely to be separated with similar resolution by thermal desorption methods. The increase in dicarboxylic acid signal with increasing carbon number up to sebacic acid in Fig. 2 is the opposite of the trend observed by Lee et al. (2014) for direct evaporation of succinic, glutaric, adipic, and azelaic acid into a I-CIMS. This suggests that the signals observed here may have been influenced by the HPLC and/or VIA, perhaps due to differences in the composition of solvent drops exiting the HPLC or other factors that might affect evaporation, decomposition, and wall loss in the VIA. This could be investigated in the future by, for example, using isocratic HPLC, varying the vaporizer temperature, and measuring the aerosol size distribution.

Table 1: Calibration curve linearity and sensitivity for 12 carboxylic acid standards. Compounds are arranged in ascending order of retention time.

| Compound | Formula | Linearity (R ²) | Sensitivity (area/nmol x 10 ³) |
|-------------------------|---------------------|-----------------------------|--|
| Adipic Acid | $C_6H_{10}O_4$ | 0.996 | 7.01 |
| Pimelic Acid | $C_7H_{12}O_4$ | 0.992 | 10.7 |
| Suberic Acid | $C_8H_{14}O_4$ | 0.989 | 18.1 |
| Azelaic Acid | $C_9H_{16}O_4$ | 0.976 | 32.4 |
| Sebacic Acid | $C_{10}H_{18}O_4$ | 0.991 | 27.2 |
| Undecanedioic Acid | $C_{11}H_{20}O_4$ | 0.991 | 27.5 |
| Dodecanedioic Acid | $C_{12}H_{22}O_4$ | 0.992 | 14.4 |
| 16-Hydroxypalmitic Acid | $C_{16}H_{32}O_3$ | 0.989 | 44.6 |
| 12-Hydroxystearic Acid | $C_{18}H_{36}O_{3}$ | 0.980 | 98.6 |
| 2-Hydroxypalmitic Acid | $C_{16}H_{32}O_3$ | 0.986 | 133 |
| Palmitic Acid | $C_{16}H_{32}O_2$ | 0.973 | 2.34 |
| Stearic Acid | $C_{18}H_{36}O_2$ | 0.983 | 6.82 |

An additional advantage over separation by thermal desorption is the greater predictability of reverse-phase HPLC separation based on molecular structure. For example, when using a column that separates compounds through hydrophobic interactions (e.g., a C₈ column) the amount of interaction between analytes and the stationary phase can be inferred by both the number of polar functional groups and their relative positions. In the case of hydroxypalmitic acid, the placement of the

hydroxyl group adjacent to the carboxyl group (the 2-position) (\mathbf{B}) allows the aliphatic C_{14} chain to freely interact with the stationary phase, whereas the placement of the hydroxyl group at the 16-position (\mathbf{A}) interferes with this interaction and results in less retention on the column (Yeh and Ziemann, 2014). It is also worth noting the impact of these structural differences on the relative instrument sensitivities to \mathbf{A} and \mathbf{B} of about a factor of 3. Bi et al. observed that I-CIMS sensitivities can vary by 1–2 orders of magnitude for isomers of limonene oxidation products (Bi et al., 2021b).

200

205

215

Peak tailing was observed for most analytes and is more evident for those eluting in the latter half of the analysis. While total signal appeared to depend on the flow rate through the nebulizer bulb and VIA, peak shape did not (Fig. S2), indicating instead an upstream influence of the HPLC column or tubing. Comparing the results obtained here with those observed by Yeh and Ziemann (2014) and Schueneman et al. (2024), who used a similar system consisting of an HPLC coupled with TDPBMS and EESI-MS using a Collison atomizer, it is clear that the HPLC-VIA-CIMS provides better preservation of chromatographic peak shape between the HPLC and MS detection.

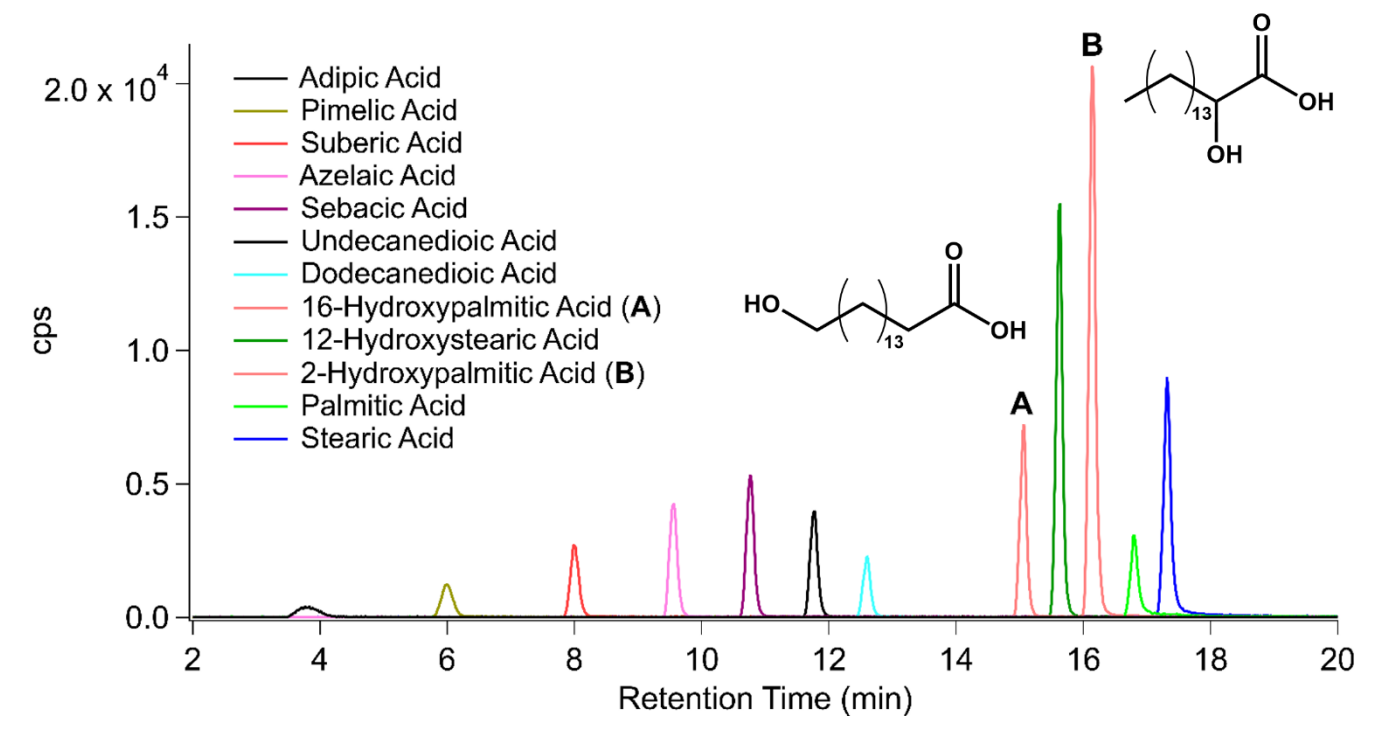


Figure 2: HPLC-VIA-CIMS extracted ion chromatogram of a mixture containing 12 organic acid standards. The injection quantity was 1.5 nmol for each standard except for palmitic acid and stearic acid, which were 15 nmol each. The structures of 16-hydroxypalmitic acid (A) and 2-hydroxypalmitic acid (B) are included for clarity.

Thermal decomposition of compounds in the VIA has been previously reported as a limitation of this inlet (Häkkinen et al., 2023). If sufficient analyte separation is achieved by the HPLC, then all detectable thermal decomposition products can be attributed to the respective precursor ion based on retention time alignment. This feature would prove useful for the analysis of thermally labile compounds by HPLC-VIA-CIMS, such as multifunctional nitrates and peroxide-containing reaction products. Evidence of thermal decomposition was not observed for the carboxylic acid standards examined here, perhaps

because of negligible decomposition or because the iodide reagent ion is not sensitive to the decomposition products. Full characterization of thermal decomposition is beyond the scope of this work, but it can be minimized by operating the VIA at lower temperatures or reducing residence time (Zhao et al., 2024).

To evaluate the linearity of the HPLC-VIA-CIMS response, seven-point calibration curves were generated with injection ranges of 0.2-3.0 nmol for all standards except for palmitic acid and stearic acid, for which a range of 2-30 nmol was used. The results are shown in Table 1. The system was found to have a linear response for all analytes ($R^2 > 0.97$) across the tested range of mass loadings, illustrating the potential of the HPLC-VIA-CIMS to be used for quantitation of analytes for which authentic standards can be purchased or synthesized. Calibration curves for each analyte are shown in Fig. S1.

3.2 \alpha-Pinene Ozonolysis SOA

220

225

230

235

240

245

SOA formed by ozonolysis of α-pinene was chosen for method evaluation with a complex OA as it has been well characterized and is known to contain carboxylic acid monomer and dimer products that are detected by I-CIMS with high sensitivity (Lopez-Hilfiker et al., 2014) and are often isobaric or differ by only two hydrogen atoms (Ma et al., 2007a; Zhao et al., 2024). Although other classes of compounds may co-elute with these (~2000 compounds have been detected in this type of SOA; Heaton et al., 2009), they would need to have very similar chromatographic properties and be present in high abundance to compensate for the much lower detection sensitivity. Analysis of a 30 μg injection of the SOA by HPLC-VIA-CIMS identified numerous products, but for clarity a subset of these was selected here (and in the section below) based on relative contributions to the total I-CIMS signal (Fig. S3 and Fig. S4) and prevalence in the literature to illustrate the performance of the HPLC-VIA-CIMS system. Although a comprehensive analyte list was not compiled, the diversity of compounds detected by this system can be seen in the averaged mass spectra shown in Fig. S4 and Fig. S6. These spectra provide a qualitative view of the numerous other analytes detected in the mass range that was measured. It should be noted that the number of detectable compounds is more likely to be limited by injection mass rather than total collected aerosol mass.

Chromatograms are shown in Fig. 3 and are divided into monomers (C_{8-10}) and dimers (C_{17-19}). The $C_8H_{12}O_4$ (second peak, 9 min) and $C_{10}H_{16}O_3$ (12.5 min) monomers were confirmed to be *trans*-norpinic acid and *cis*-pinonic acid, respectively, by comparing the retention times and peak shapes to those of authentic standards (Fig. S5). This suggests that these compounds and other carboxylic acids for which standards are available can be identified and quantified by HPLC-VIA-CIMS. A larger $C_8H_{12}O_4$ peak was observed at a retention time of 7 min, which may be terpenylic acid as it is known to be produced by α -pinene ozonolysis in high yield (Claeys et al., 2009). And it is likely that *cis*-pinic acid ($C_9H_{14}O_4$), a common product of α -pinene ozonolysis with a yield similar to that of *cis*-pinonic acid (Ma et al., 2007), is observed at 10.5 min. This is supported by the difference in retention time between *cis*-pinonic acid (12.5 min) and $C_9H_{14}O_4$ (10.5 min), as a more highly oxygenated compound with fewer carbon atoms would be expected to elute sooner from a reverse-phase HPLC column. A homologous series of monomer products with formulas of $C_{10}H_{16}O_{4-6}$ eluting between 8 and 13 min was also observed. Of these, $C_{10}H_{16}O_4$, corresponding to hydroxypinonic acid, and $C_{10}H_{16}O_6$, an unidentified low-volatility product, were observed to have multiple

isomers while only a single peak was detected for $C_{10}H_{16}O_5$. It has been previously shown through ion mobility measurements that structural isomers of $C_{10}H_{16}O_4$ and $C_{10}H_{16}O_6$ exist among the products of α -pinene ozonolysis (Skyttä et al., 2022).

250

255

260

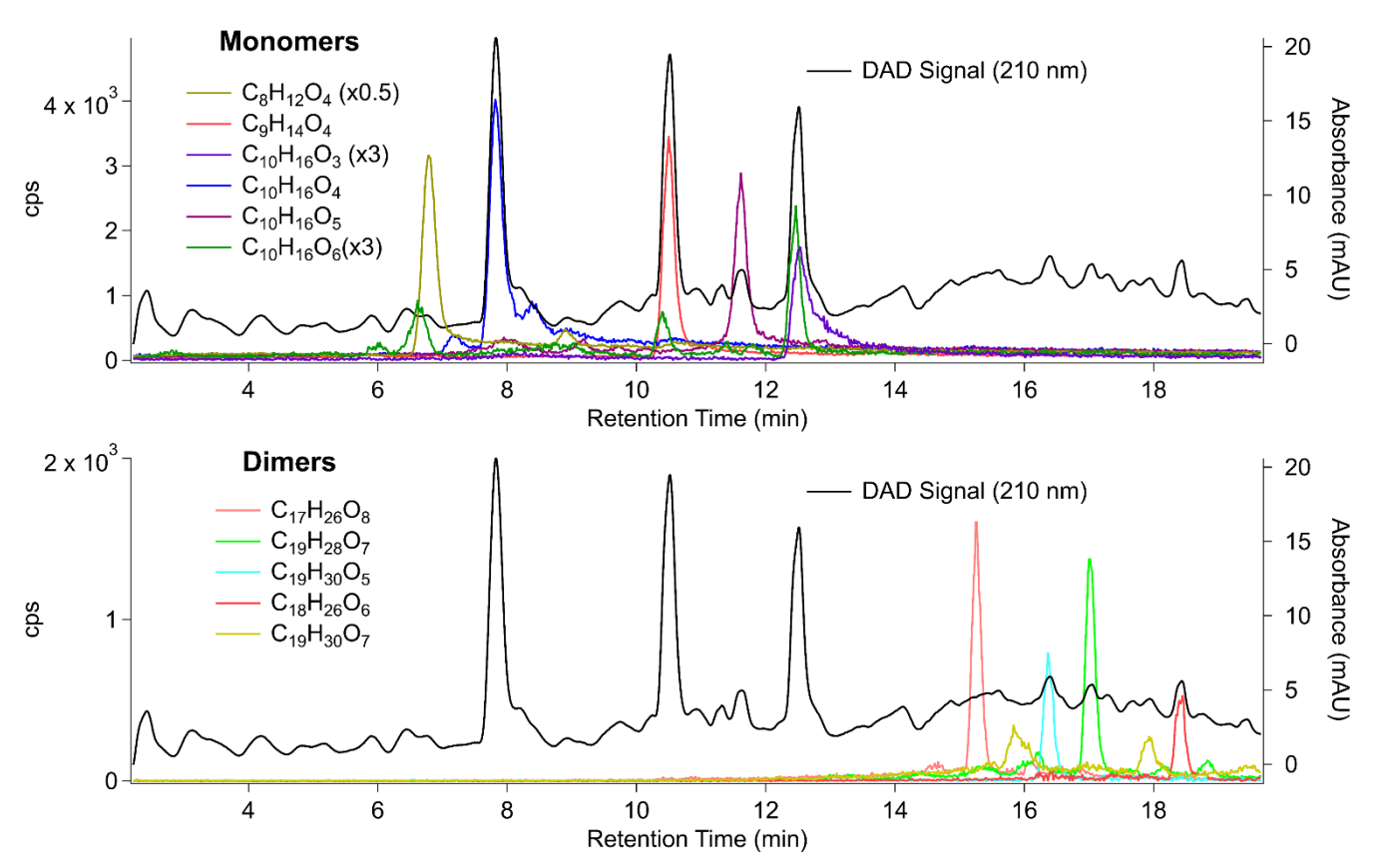


Figure 3: HPLC-VIA-CIMS extracted ion chromatograms of a 30 μ g injection of SOA generated by α -pinene ozonolysis. Monomer species (C_{8-10}) are shown in the top chromatogram and dimer species (C_{17-20}) are shown in the bottom. Compounds were detected as I^- adducts but are presented in their neutral form for clarity.

Several compounds suspected to be dimer products based on molecular formula ($C_{17-19}H_{26-30}O_{5-8}$) were detected and a subset is shown in Fig. 3. These have all been reported in other lab studies (Kenseth et al., 2023; Luo et al., 2024) and many have been observed in ambient OA (Kristensen et al., 2016). While isomeric structures of many dimer products in α -pinene ozonolysis SOA have been reported (Huang et al., 2018; Zhang et al., 2017), multiple chromatographic peaks were only observed here for $C_{19}H_{28}O_7$ and $C_{19}H_{30}O_7$. $C_{19}H_{28}O_7$ and $C_{19}H_{30}O_7$. To the authors' knowledge, isomeric structures of these species have not been explicitly described in the literature, but hypothesized dimer formation mechanisms and the diversity of monomer precursors support their identification here. It is also possible that more than one isomer of $C_{17}H_{26}O_8$, $C_{19}H_{28}O_7$, and $C_{19}H_{30}O_5$ exist in this sample but are too structurally similar to be resolved by the HPLC method that was used.

Absorbance at 210 nm was measured in addition to I-CIMS signal as monoterpene SOA has been shown to have broad absorption peaks at wavelengths below ~300 nm (Bateman et al., 2011; Bones et al., 2010) and can thus be used to

detect sufficiently absorbing species as they elute from the column. For reference, previous measurements on a series of standards determined molar absorptivities of about 4000, 200, 50, 3, and 3 M⁻¹ cm⁻¹ for a nitrate, alkenoic acid, carboxylic acid, alcohol, and ketone at 210 nm (Docherty and Ziemann, 2006). After retention time alignment with the I-CIMS time series, the DAD signal reveals the preservation of peak shape during nebulization and evaporation in the VIA, which is most clearly observed for the peaks at 8 min (C₁₀H₁₆O₄), 10.5 min (C₉H₁₄O₄), and 12.5 min (C₁₀H₁₆O₅, C₁₀H₁₆O₆) (Fig 3, top). This is reasonable, since for a N₂ flow rate of 3.5 LPM and a bulb volume of 300 mL the residence time in the bulb is ~5 s compared to a delay time between the DAD and CIMS signals of ~2 s, indicating that most of the aerosols are rapidly transmitted through the bulb to the VIA as well-defined packets with little mixing between them due to dispersion. This point is especially important for the identification of closely related structural isomers that may otherwise be attributed to peak splitting during nebulization and evaporation of the HPLC eluent. Furthermore, for more strongly absorbing species such as nitrates, this approach may be used semi-quantitatively to determine relative abundances of closely related structures with similar molar absorptivities or, if authentic standards are available, absolute concentrations of these compounds.

3.3 Field-Collected OA

280

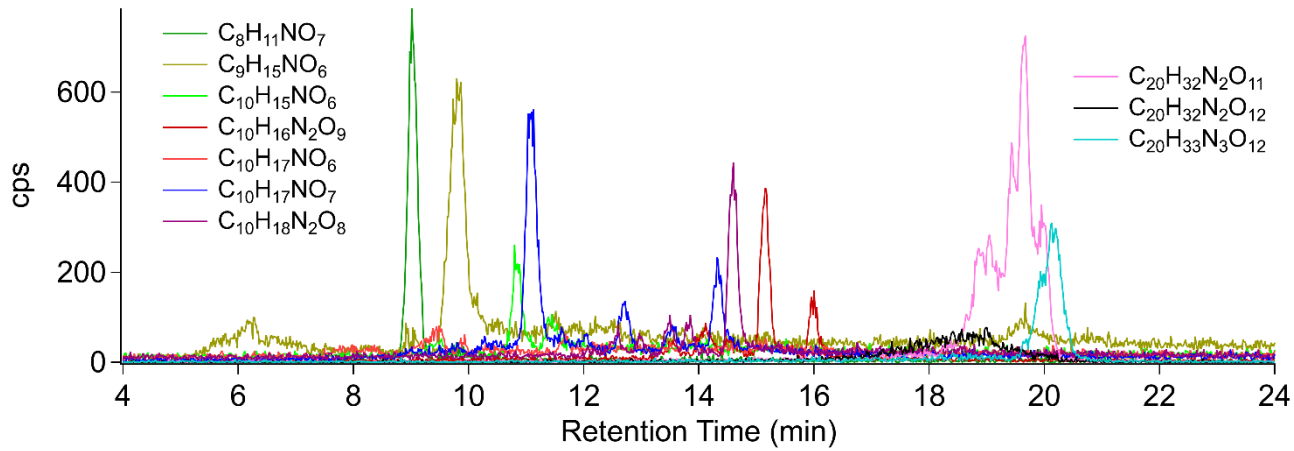
285

290

The potential application of HPLC-VIA-CIMS to field-collected SOA was evaluated by analysing an aerosol sample collected at the Denver, Colorado ASCENT site. Aerosol from this site was chosen as it was likely to contain multifunctional nitrates, which are easily detected by I-CIMS (He et al., 2024) and often occur as mixtures of isomers. The chromatogram generated from a 60 µg injection of this sample is shown in Fig. 4 and includes several compounds with molecular formulas that are consistent with multifunctional nitrates formed through monoterpene oxidation in an urban environment. The detection of these compounds is unsurprising given the prevalence of monoterpenes in the Denver area from biogenic emissions, personal care products, and cannabis cultivation and other sources (La Casa | ASCENT, 2024; Gkatzelis et al., 2021; Wang et al., 2020). Although this analysis only highlights this subset of compounds, numerous other species were detected by HPLC-VIA-CIMS and are shown in Fig. S6 in the Supplemental.

Compounds suspected to be monoterpene oxidation products consisted of C_{8-9} species (assumed to be products of monomer decomposition reactions), C_{10} monomers, and C_{20} dimers. Specifically, $C_8H_{11}NO_7$, $C_9H_{15}NO_6$, $C_{10}H_{16}N_2O_9$, and $C_{10}H_{18}N_2O_9$ have been detected as products of the reaction of limonene with nitrate radicals (Faxon et al., 2018), whereas $C_{10}H_{15}NO_6$, $C_{10}H_{17}NO_6$, and $C_{10}H_{17}NO_7$ are consistent with products formed through the oxidation of limonene and other monoterpenes by either nitrate radicals (DeVault et al., 2022b) or by hydroxyl radicals in the presence of NO_x (DeVault et al., 2022a). It is worth noting the complex peak shapes of $C_{10}H_{17}NO_7$ and $C_{10}H_{16}N_2O_9$ eluting between 11 and 16 min. Considering

the ability of the nebulizer-VIA interface to transfer analytes from the HPLC to the I-CIMS with minimal peak distortion, it can be asserted that these peak shapes indicate the presence of multiple isomers and are not artifacts.



295 Figure 4: HPLC-VIA-CIMS extracted ion chromatogram of a 60 μg injection of ambient SOA collected at the Denver, Colorado ASCENT site. The chemical formulas shown do not include I but were detected as I adducts.

Three dimer species, $C_{20}H_{32}N_2O_{11}$, $C_{20}H_{32}N_2O_{12}$, and $C_{20}H_{32}N_3O_{12}$, were attributed to particle-phase accretion reactions of monomers formed through the reaction of monoterpenes with nitrate radicals (DeVault et al., 2022b; Faxon et al., 2018; Takeuchi et al., 2022). Complex peak shapes were observed for $C_{20}H_{32}N_2O_{11}$ and $C_{20}H_{33}N_3O_{12}$ beginning at retention times of 18 and 19.5 min, respectively, suggesting the presence of multiple isomers. This is reasonable given the detection of monomer isomers and the possibility that these products were formed by several different monoterpene precursors. Multiple isomers of $C_{20}H_{33}N_3O_{12}$ were proposed by Takeuchi et al. (2022) in a study of nitrate radical oxidation of α -pinene/limonene mixtures, further supporting the assignment of these peaks.

300

305

310

315

The prevalence of organic nitrates and absence of carboxylic acid products of monoterpene ozonolysis is likely due to the nighttime and daytime oxidation conditions under which the SOA was formed. As shown in Fig. S7, in the nighttime hours before sampling began, the O_3 , NO_2 , and NO concentrations were about 20, 10, and 0 ppb due to titration of NO to NO_2 by reaction with O_3 . Although concentrations of NO_3 radicals formed by the $NO_2 + O_3 \rightarrow NO_3 + O_2$ reaction were not measured, values of <0.5-100 ppt have been reported at field sites impacted by the Denver urban plume (Brown and Stutz, 2012). Given a k_{NO_3}/k_{O_3} rate constant ratio of about 7×10^4 for common monoterpenes such as limonene and α -pinene (Atkinson and Arey, 2003) and an assumed minimum $[NO_3]/[O_3]$ ratio of 1 ppt/20 ppb = 5×10^{-5} , the minimum fraction of monoterpenes that would react with NO_3 radicals would be $\sim 75\%$, indicating that formation of organic nitrates by these reactions should dominate the fate of monoterpenes during this period. As NO concentrations increase at about 05:00 as rush hour begins, NO_3 radicals will be removed by the $NO_3 + NO \rightarrow 2NO_2$ reaction. Alkylperoxy radicals formed by reactions of monoterpenes with O_3 and OH radicals formed by ozonolysis or by photolysis after sunrise at 07:00 (which will also photolyze NO_3 radicals) will then react with NO to form organic nitrates and few carboxylic acids. The detection of $C_{10}H_yNO_x$ species in the OA samples is also consistent with measurements by Lee et al. (2016), who described a diurnal pattern of monoterpene-derived multifunctional

alkyl nitrates, with concentrations peaking in the early morning hours, in the southeast United States. Although their real-time measurements combined with modelling indicated lifetimes of 2–4 h, previous studies by DeVault and Ziemann (2021) and DeVault et al. (2022a, 2022b) showed that organic nitrates formed from monoterpene oxidation reactions were stable for at least several days after filter sampling and extraction processes similar to those used here. While it is possible that some of the CHNO species are not organic nitrates, our results shown in Figures 4 and S6 are consistent with the C₁₀ organic nitrate distributions observed by Lee et al. (2016) during the early morning hours of their study period.

4 Conclusions

320

325

330

335

340

We have described and evaluated the coupling of an HPLC and an I-CIMS for measurement of environmental chambergenerated and field-collected OA. The HPLC-VIA-CIMS achieved excellent separation of carboxylic acids, dicarboxylic acids, and hydroxycarboxylic acids, including a pair of structural isomers, while also having a linear response to analyte mass over an order of magnitude. The system also provided isomer-resolved detection of α -pinene ozonolysis products, including both monomer and dimer species that have been reported in previous studies of this reaction. Detection of these compounds by a DAD provided evidence for high-fidelity transmission of chromatographic peaks from the HPLC to the I-CIMS. In future work, the DAD could be used to provide semi-quantitative analysis of light-absorbing compounds for which standards are not available. This may prove particularly advantageous for chamber studies as HPLC-VIA-CIMS would enable direct measurements of species-specific particle-phase product yields, including yields of organic nitrates, which are important since they impact loss rates of gas-phase reactive nitrogen and therefore ozone formation. Although outside the scope of the present study, this apparatus could also be used to systematically evaluate possible artifacts incurred by filter sampling and other sample handling procedures used in off-line analysis by comparing averaged mass spectra generated with HPLC-VIA-CIMS with those from online VIA-CIMS measurements. Analysis of field-collected OA by HPLC-VIA-CIMS produced similarly promising results, including the detection of several nitrogen-containing compounds attributed to monoterpene oxidation products. Even at low mass loadings (<100 μg OA extract), excellent signal strength was achieved for numerous nitrate compounds, illustrating the potential of the HPLC-VIA-CIMS to be used in studies of ambient aerosol composition, especially if detection limits can be lowered. This might be accomplished, for example, by improving the nebulizer design to increase transmission or by using other CIMS reagent ions that have higher sensitivity to compounds of interest. Finally, using HPLC-VIA-CIMS to characterize SOA enables direct comparison with gas-phase species that are also detected using CIMS, simplifying investigations of semivolatile compounds present in the atmosphere.

345 Data availability. Data for this work is available upon request.

Supplement.

Author Contributions. AFS and PJZ conceptualized the project. AFS developed the nebulizer interface, performed the chamber experiment, sample preparation, and data analysis, generated the figures and tables, and wrote the paper. KHB reviewed and edited the paper. KEM provided guidance on laboratory experiments and also reviewed the paper. ERL organized the ambient SOA sample collection and FM processed the sample. MRC and MWA provided the VIA, assisted with VIA operation, and reviewed the paper.

355 Competing Interests. MRC and MWA are employees of Aerodyne Research Inc., which sells the VIA.

Financial Support. This material is based on work supported by the National Science Foundation under grant AGS-1750447.

References

380

- Aljawhary, D., Lee, A. K. Y., and Abbatt, J. P. D.: High-resolution chemical ionization mass spectrometry (ToF-CIMS):
- Application to study SOA composition and processing, Atmos. Meas. Tech., 6, 3211–3224, https://doi.org/10.5194/amt-6-3211-2013, 2013.
 - Alton, M., Canagaratna, M., Avery, A., Lambe, A., Kangasluoma, J., Ehn, M., Mickwitz, V., Zhao, J., and Worsnop, D.: Measurements of atmospheric aerosol with the vaporization inlet for aerosols and the filter inlet for gases and aerosols on a bipolar multi-reagent chemical ionization mass spectrometer, EGU General Assembly 2024, Vienna, Austria, 14–19 Apr 2024,
- 365 EGU24-12470, https://doi.org/10.5194/egusphere-egu24-12470, 2024.
 - Apffel, A., Fischer, S., Goldberg, G., Goodley, P. C., and Kuhlmann, F. E.: Enhanced sensitivity for peptide mapping with electrospray liquid chromatography-mass spectrometry in the presence of signal suppression due to trifluoroacetic acid-containing mobile phases, J. Chromatogr. A., 712, 177-190, https://doi.org/10.1016/0021-9673(95)00175-M, 1995.
- Atkinson, R. and Arey, J.: Atmospheric degradation of volatile organic compounds, Chem. Rev., 103, 4605–4638, https://doi.org/10.1021/cr0206420, 2003.
 - Bateman, A. P., Nizkorodov, S. A., Laskin, J., and Laskin, A.: Photolytic processing of secondary organic aerosols dissolved in cloud droplets, Phys. Chem. Chem. Phys., 13, 12199–12212, https://doi.org/10.1039/c1cp20526a, 2011.
 - Bi, C., Krechmer, J. E., Frazier, G. O., Xu, W., Lambe, A. T., Claflin, M. S., Lerner, B. M., Jayne, J. T., Worsnop, D. R., Canagaratna, M. R., and Isaacman-Vanwertz, G.: Coupling a gas chromatograph simultaneously to a flame ionization detector
- and chemical ionization mass spectrometer for isomer-resolved measurements of particle-phase organic compounds, Atmos. Meas. Tech., 14, 3895–3907, https://doi.org/10.5194/amt-14-3895-2021, 2021a.
 - Bi, C., Krechmer, J. E., Frazier, G. O., Xu, W., Lambe, A. T., Claflin, M. S., Lerner, B. M., Jayne, J. T., Worsnop, D. R., Canagaratna, M. R., and Isaacman-Vanwertz, G.: Quantification of isomer-resolved iodide chemical ionization mass spectrometry sensitivity and uncertainty using a voltage-scanning approach, Atmos. Meas. Tech., 14, 6835–6850, https://doi.org/10.5194/amt-14-6835-2021, 2021b.
 - Bones, D. L., Henricksen, D. K., Mang, S. A., Gonsior, M., Bateman, A. P., Nguyen, T. B., Cooper, W. J., and Nizkorodov, S. A.: Appearance of strong absorbers and fluorophores in limonene-O₃ secondary organic aerosol due to NH4+ -mediated chemical aging over long time scales, J. Geophys. Res. Atmos., 115, D05203, https://doi.org/10.1029/2009JD012864, 2010.
- Brown, S. S. and Stutz, J.: Nighttime radical observations and chemistry, Chem. Soc. Rev., 41, 6405–6447, https://doi.org/10.1039/c2cs35181a, 2012.
 - Cai, J., Daellenbach, K. R., Wu, C., Zheng, Y., Zheng, F., Du, W., Haslett, S. L., Chen, Q., Kulmala, M., and Mohr, C.: Characterization of offline analysis of particulate matter with FIGAERO-CIMS, Atmos. Meas. Tech., 16, 1147–1165, https://doi.org/10.5194/amt-16-1147-2023, 2023.
 - Canagaratna, M. R., Jayne, J. T., Jimenez, J. L., Allan, J. D., Alfarra, M. R., Zhang, Q., Onasch, T. B., Drewnick, F., Coe, H.,
- 390 Middlebrook, A., Delia, A., Williams, L. R., Trimborn, A. M., Northway, M. J., DeCarlo, P. F., Kolb, C. E., Davidovits, P.,

- and Worsnop, D. R.: Chemical and microphysical characterization of ambient aerosols with the aerodyne aerosol mass spectrometer, Mass Spectrom. Rev., 26, 185–222, https://doi.org/10.1002/mas.20115, 2007.
- Claeys, M., Iinuma, Y., Szmigielski, R., Surratt, J. D., Blockhuys, F., Van Alsenoy, C., Böge, O., Sierau, B., Gómez-González, Y., Vermeylen, R., Van Der Veken, P., Shahgholi, M., Chan, A. W. H., Herrmann, H., Seinfeld, J. H., and Maenhaut, W.:
- 395 Terpenylic acid and related compounds from the oxidation of α-pinene: Implications for new particle formation and growth above forests, Environ. Sci. Technol., 43, 6976–6982, https://doi.org/10.1021/es9007596, 2009.
 - Claflin, M. S. and Ziemann, P. J.: Thermal desorption behavior of hemiacetal, acetal, ether, and ester oligomers, Aerosol Sci. Tech., 53, 473–484, https://doi.org/10.1080/02786826.2019.1576853, 2019.
- Devault, M. P. and Ziemann, P. J.: Gas- and particle-phase products and their mechanisms of formation from the reaction of Δ-3-carene with NO₃ radicals, J. Phys. Chem. A., 125, 10207-10222, https://doi.org/10.1021/acs.jpca.1c07763, 2021.
- Devault, M. P., Ziola, A. C., and Ziemann, P. J.: Chemistry of secondary organic aerosol formation from reactions of monoterpenes with OH radicals in the presence of NO_x, J. Phys. Chem. A, 126, 7719–7736, https://doi.org/10.1021/acs.jpca.2c04605, 2022a.
 - Devault, M. P., Ziola, A. C., and Ziemann, P. J.: Products and mechanisms of secondary organic aerosol formation from the
- NO₃ radical-initiated oxidation of cyclic and acyclic monoterpenes, ACS Earth Space Chem., 6, 2076–2092, https://doi.org/10.1021/acsearthspacechem.2c00130, 2022b.
 - Docherty, K. S. and Ziemann, P. J.: Reaction of oleic acid particles with NO₃ radicals: Products, mechanism, and implications for radical-initiated organic aerosol oxidation, J. Phys. Chem. A, 110, 3567–3577, https://doi.org/10.1021/jp0582383, 2006.
 - Docherty, K. S., Kumboonlert, K., Lee, I. J., and Ziemann, P. J.: Gas chromatography of trimethylsilyl derivatives of α-
- 410 methoxyalkyl hydroperoxides formed in alkene-O₃ reactions, J. Chromatogr. A., 1029, 205–215, https://doi.org/10.1016/j.chroma.2003.12.014, 2004.
 - Eichler, P., Müller, M., D'Anna, B., and Wisthaler, A.: A novel inlet system for online chemical analysis of semi-volatile submicron particulate matter, Atmos. Meas. Tech., 8, 1353–1360, https://doi.org/10.5194/amt-8-1353-2015, 2015.
- Faxon, C., Hammes, J., Le Breton, M., Pathak, R. K., and Hallquist, M.: Characterization of organic nitrate constituents of secondary organic aerosol (SOA) from nitrate-radical-initiated oxidation of limonene using high-resolution chemical

ionization mass spectrometry, Atmos. Chem. Phys., 18, 5467–5481, https://doi.org/10.5194/acp-18-5467-2018, 2018.

- Finewax, Z., Jimenez, J. L., and Ziemann, P. J.: Development and application of a low-cost vaporizer for rapid, quantitative, in situ addition of organic gases and particles to an environmental chamber, Aerosol Sci. Tech., 54, 1567–1578, https://doi.org/10.1080/02786826.2020.1808186, 2020.
- 420 Goldstein, A. H. and Galbally, I. E.: Known and unexplored organic constituents in the earth's atmosphere, Environ. Sci. Technol., 41, 1514–1521, https://doi.org/10.1021/es072476p, 2007.
 - Häkkinen, E., Zhao, J., Graeffe, F., Fauré, N., Krechmer, J. E., Worsnop, D., Timonen, H., Ehn, M., and Kangasluoma, J.: Online measurement of highly oxygenated compounds from organic aerosol, Atmos. Meas. Tech., 16, 1705–1721, https://doi.org/10.5194/amt-16-1705-2023, 2023.

- He, S., Liu, Y., Song, M., Li, X., Lou, S., Ye, C., Liu, Y., Liu, Y., Ye, J., Lu, S., Zhou, W., Qiu, X., Zhu, T., and Zeng, L.: Empirical approach to quantifying sensitivity in different chemical ionization techniques for organonitrates and nitroaromatics constrained by ion-molecule reaction and transmission efficiency, Anal. Chem., https://doi.org/10.1021/acs.analchem.4c03751, 96, 16882–16890 2024.
 - Hearn, J. D. and Smith, G. D.: A chemical ionization mass spectrometry method for the online analysis of organic aerosols,
- $430 \quad Anal. \ Chem., \ 76, \ 2820-2826, \ https://doi.org/10.1021/ac049948s, \ 2004.$
 - Heaton, K. J., Sleighter, R. L., Hatcher, P. G., Hall IV, W. A., and Johnston, M. V.: Composition domains in monoterpene secondary organic aerosol, Environ. Sci. Technol., 43, 7797–7802, https://doi.org/10.1021/es901214p, 2009.
 - Hildmann, S. and Hoffmann, T.: Characterisation of atmospheric organic aerosols with one- and multidimensional liquid chromatography and mass spectrometry: State of the art and future perspectives, Trends Anal. Chem., 175, 117698,
- 435 https://doi.org/10.1016/j.trac.2024.117698, 2024.
 - Hoffmann, T., Bandur, R., Marggraf, U., and Linscheid, M.: Molecular composition of organic aerosols formed in the α-pinene/O₃ reaction: Implications for new particle formation processes, J. Geophys. Res. Atmos., 103, 25569–25578, https://doi.org/10.1029/98JD01816, 1998.
- Huang, W., Saathoff, H., Pajunoja, A., Shen, X., Naumann, K. H., Wagner, R., Virtanen, A., Leisner, T., and Mohr, C.: α-
- Pinene secondary organic aerosol at low temperature: Chemical composition and implications for particle viscosity, Atmos. Chem. Phys., 18, 2883–2898, https://doi.org/10.5194/acp-18-2883-2018, 2018.
 - Kenseth, C. M., Hafeman, N. J., Rezgui, S. P., Chen, J., Huang, Y., Dalleska, N. F., Kjaergaard, H. G., Stoltz, B. M., Seinfeld, J. H., and Wennberg, P. O.: Particle-phase accretion forms dimer esters in pinene secondary organic aerosol, Science, 382, 787–792, https://doi.org/10.1126/science.adi0857, 2023.
- Krechmer, J. E., Groessl, M., Zhang, X., Junninen, H., Massoli, P., Lambe, A. T., Kimmel, J. R., Cubison, M. J., Graf, S., Lin, Y. H., Budisulistiorini, S. H., Zhang, H., Surratt, J. D., Knochenmuss, R., Jayne, J. T., Worsnop, D. R., Jimenez, J. L., and Canagaratna, M. R.: Ion mobility spectrometry-mass spectrometry (IMS-MS) for on- and offline analysis of atmospheric gas and aerosol species, Atmos. Meas. Tech., 9, 3245–3262, https://doi.org/10.5194/amt-9-3245-2016, 2016.
 - Gkatzelis, G. I., Coggon, M. M., McDonald, B. C., Peischl, J., Aikin, K. C., Gilman, J. B., Trainer, M., and Warneke, C.:
- 450 Identifying volatile chemical product tracer compounds in U.S. cities, Environ. Sci. Technol., 55, 188-199, https://dx.doi.org/10.1021/acs.est.0c05467?ref=pdf, 2021.
 - Kristensen, K., Watne, Å. K., Hammes, J., Lutz, A., Petäjä, T., Hallquist, M., Bilde, M., and Glasius, M.: High-molecular weight dimer esters are major products in aerosols from α-pinene ozonolysis and the boreal forest, Environ. Sci. Technol. Lett., 3, 280–285, https://doi.org/10.1021/acs.estlett.6b00152, 2016.
- Kroll, J. H. and Seinfeld, J. H.: Chemistry of secondary organic aerosol: Formation and evolution of low-volatility organics in the atmosphere, Atmos. Environ., 42, 3593–3624, https://doi.org/10.1016/j.atmosenv.2008.01.003, 2008.
 La Casa | ASCENT: https://ascent.research.gatech.edu/la-casa, last access: 9 December 2024.

- Lee, B. H., Lopez-Hilfiker, F. D., Mohr, C., Kurtén, T., Worsnop, D. R., and Thornton, J. A.: An iodide-adduct high-resolution time-of-flight chemical-ionization mass spectrometer: Application to atmospheric inorganic and organic compounds, Environ.
- 460 Sci. Technol., 48, 6309–6317, https://doi.org/10.1021/es500362a, 2014.
 - Lee, B. H., Mohr, C., Lopez-Hilfiker, F. D., and Thornton, J. A.: Highly functionalized organic nitrates in the southeast united states: contribution to secondary organic aerosol and reactive nitrogen budgets, PNAS, 113, 1516-1521, https://doi.org/10.1073/pnas.1508108113, 2016.
 - Lobrutto, R., Jones, A., Kazakevich, Y. V, and Mcnair, H. M.: Effect of the eluent pH and acidic modifiers in high-performance
- 465 liquid chromatography retention of basic analytes, J. Chromatogr. A, 913, 173–187, https://doi.org/10.1016/S0021-9673(00)01012-8, 2001.
 - Lopez-Hilfiker, F. D., Mohr, C., Ehn, M., Rubach, F., Kleist, E., Wildt, J., Mentel, T. F., Lutz, A., Hallquist, M., Worsnop, D., and Thornton, J. A.: A novel method for online analysis of gas and particle composition: Description and evaluation of a filter inlet for gases and aerosols (FIGAERO), Atmos. Meas. Tech., 7, 983–1001, https://doi.org/10.5194/amt-7-983-2014,
- 470 2014.
 - Luo, H., Guo, Y., Shen, H., Huang, D. D., Zhang, Y., and Zhao, D.: Effect of relative humidity on the molecular composition of secondary organic aerosols from α-pinene ozonolysis, Environ. Sci.: Atmos., 4, 519–530, https://doi.org/10.1039/d3ea00149k, 2024.
- Ma, Y., Luciani, T., Porter, R. A., Russell, A. T., Johnson, D., and Marston, G.: Organic acid formation in the gas-phase ozonolysis of α-pinene, Phys. Chem. Chem. Phys., 9, 5084–5087, https://doi.org/10.1039/b709880d, 2007a.
 - Ma, Y., Willcox, T. R., Russell, A. T., and Marston, G.: Pinic and pinonic acid formation in the reaction of ozone with α-pinene, Chem. Commun., 1328–1330, https://doi.org/10.1039/b617130c, 2007b.
 - Mauderly, J. L. and Chow, J. C.: Health effects of organic aerosols, Inhal. Toxicol., 20, 257–288, https://doi.org/10.1080/08958370701866008, 2008.
- Pöschl, U.: Atmospheric aerosols: Composition, transformation, climate and health effects, Angew. Chem. Int. Ed., 44, 7520–7540, https://doi.org/10.1002/anie.200501122, 2005.
 - Reinnig, M. C., Müller, L., Warnke, J., and Hoffmann, T.: Characterization of selected organic compound classes in secondary organic aerosol from biogenic VOCs by HPLC/MSn, Anal. Bioanal. Chem., 391, 171–182, https://doi.org/10.1007/s00216-008-1964-5, 2008.
- Riva, M., Pospisilova, V., Frege, C., Perrier, S., Bansal, P., Jorga, S., Sturm, P., Thornton, J. A., Rohner, U., and Lopez-Hilfiker, F.: Evaluation of a reduced-pressure chemical ion reactor utilizing adduct ionization for the detection of gaseous organic and inorganic species, Atmos. Meas. Tech., 17, 5887–5901, https://doi.org/10.5194/amt-17-5887-2024, 2024.
 - Robinson, M. A., Roberts, J. M., Neuman, J. A., Jernigan, C. M., Xu, L., Coggon, M. M., Stockwell, C. E., Warneke, C., Peischl, J., Gilman, J. B., Lamplugh, A., Rollins, A. W., Zuraski, K., Rivera-Rios, J. C., Wang, Y., Ng, N. L., Liu, S., Brown,
- 490 S. S., and Veres, P. R.: Online calibration of a chemical ionization mass spectrometer for multifunctional biogenic organic nitrates, ACS ES&T Air, 1, 1066–1083, https://doi.org/10.1021/acsestair.4c00056, 2024.

- Ruiz-Jiménez, J., Hautala, S., Parshintsev, J., Laitinen, T., Hartonen, K., Petäjä, T., Kulmala, M., and Riekkola, M. L.: Aliphatic and aromatic amines in atmospheric aerosol particles: comparison of three ionization techniques in liquid chromatography-mass spectrometry and method development, Talanta, 97, 55–62,
- Schueneman, M. K., Day, D. A., Kim, D., Campuzano-Jost, P., Yun, S., DeVault, M. P., Ziola, A. C., Ziemann, P. J., and Jimenez, J. L.: A multi-instrumental approach for calibrating real-time mass spectrometers using high-performance liquid chromatography and positive matrix factorization, Aerosol Research, 2, 59–76, https://doi.org/10.5194/ar-2-59-2024, 2024.

495

515

https://doi.org/10.1016/j.talanta.2012.03.062, 2012.

https://doi.org/10.1016/j.atmosenv.2020.117510, 2020.

- Schwarzenbach, R.: High-performance liquid chromatography of carboxylic acids, J. Chromatogr. A, 251, 339–358, https://doi.org/10.1016/S0021-9673(00)87024-7, 1982.
 - Shrivastava, M., Cappa, C. D., Fan, J., Goldstein, A. H., Guenther, A. B., Jimenez, J. L., Kuang, C., Laskin, A., Martin, S. T., Ng, N. L., Petaja, T., Pierce, J. R., Rasch, P. J., Roldin, P., Seinfeld, J. H., Shilling, J., Smith, J. N., Thornton, J. A., Volkamer, R., Wang, J., Worsnop, D. R., Zaveri, R. A., Zelenyuk, A., and Zhang, Q.: Recent advances in understanding secondary organic aerosol: implications for global climate forcing, Rev. Geophys., 55, 509–559, https://doi.org/10.1002/2016RG000540, 2017.
- 505 Skyttä, A., Gao, J., Cai, R., Ehn, M., Ahonen, L. R., Kurten, T., Wang, Z., Rissanen, M. P., and Kangasluoma, J.: Isomerresolved mobility-mass analysis of α-pinene ozonolysis products, J. Phys. Chem. A, 126, 5040–5049, https://doi.org/10.1021/acs.jpca.2c03366, 2022.
 - Takeuchi, M., Berkemeier, T., Eris, G., and Ng, N. L.: Non-linear effects of secondary organic aerosol formation and properties in multi-precursor systems, Nat. Commun., 13, https://doi.org/10.1038/s41467-022-35546-1, 2022.
- Vasquez, K. T., Allen, H. M., Crounse, J. D., Praske, E., Xu, L., Noelscher, A. C., and Wennberg, P. O.: Low-pressure gas chromatography with chemical ionization mass spectrometry for quantification of multifunctional organic compounds in the atmosphere, Atmos. Meas. Tech., 11, 6815–6832, https://doi.org/10.5194/amt-11-6815-2018, 2018.
 - Voisin, D., Smith, J. N., Sakurai, H., McMurry, P. H., and Eisele, F. L.: Thermal desorption chemical ionization mass spectrometer for ultrafine particle chemical composition, Aerosol Sci. Tech., 37, 471–475, https://doi.org/10.1080/02786820300959, 2003.
- Wang, C. T., Ashworth, K., Wiedinmyer, C., Ortega, J., Harley, P. C., Rasool, Q. Z., and Vizuete, W.: Ambient measurements of monoterpenes near cannabis cultivation facilities in Denver, Colorado, Atmos. Environ., 232,
- Warneke, C., De Gouw, J. A., Kuster, W. C., Goldan, P. D., and Fall, R.: Validation of atmospheric VOC measurements by proton-transfer-reaction mass spectrometry using a gas-chromatographic preseparation method, Environ. Sci. Technol., 37, 2494–2501, https://doi.org/10.1021/es026266i, 2003.
 - Warscheid, B. and Hoffmann, T.: On-line measurements of α -pinene ozonolysis products using an atmospheric pressure chemical ionisation ion-trap mass spectrometer, Atmos. Environ., 35, 2927–2940, https://doi.org/10.1016/S1352-2310(00)00513-6, 2001.

- Yeh, G. K. and Ziemann, P. J.: Identification and yields of 1,4-hydroxynitrates formed from the reactions of C₈-C₁₆ n-alkanes with OH radicals in the presence of NOx, J. Phys. Chem. A, 118, 8797–8806, https://doi.org/10.1021/jp505870d, 2014.
 - Yu, J., Flagan, R. C., and Seinfeld, J. H.: Identification of products containing -COOH, -OH, and -C=O in atmospheric oxidation of hydrocarbons, Environ. Sci. Technol., 32, 2357–2370, https://doi.org/10.1021/es980129x, 1998.
- Yu, J., Griffin, R. J., Cocker, D. R., Flagan, R. C., Seinfeld, J. H., and Blanchard, P.: Observation of gaseous and particulate products of monoterpene oxidation in forest atmospheres, Geophys. Res. Lett., 26, 1145–1148, https://doi.org/10.1029/1999GL900169, 1999.
 - Zhang, X., Lambe, A. T., Upshur, M. A., Brooks, W. A., Gray Bé, A., Thomson, R. J., Geiger, F. M., Surratt, J. D., Zhang, Z., Gold, A., Graf, S., Cubison, M. J., Groessl, M., Jayne, J. T., Worsnop, D. R., and Canagaratna, M. R.: Highly oxygenated multifunctional compounds in α-pinene secondary organic aerosol, Environ. Sci. Technol., 51, 5932–5940,
- 535 https://doi.org/10.1021/acs.est.6b06588, 2017.

545

- Zhao, J., Häkkinen, E., Graeffe, F., Krechmer, J. E., Canagaratna, M. R., Worsnop, D. R., Kangasluoma, J., and Ehn, M.: A combined gas- and particle-phase analysis of highly oxygenated organic molecules (HOMs) from α-pinene ozonolysis, Atmos. Chem. Phys., 23, 3707–3730, https://doi.org/10.5194/acp-23-3707-2023, 2023.
- Zhao, J., Mickwitz, V., Luo, Y., Häkkinen, E., Graeffe, F., Zhang, J., Timonen, H., Canagaratna, M., Krechmer, J. E., Zhang,
- Q., Kulmala, M., Kangasluoma, J., Worsnop, D., and Ehn, M.: Characterization of the vaporization inlet for aerosols (VIA) for online measurements of particulate highly oxygenated organic molecules (HOMs), Atmos. Meas. Tech., 17, 1527–1543, https://doi.org/10.5194/amt-17-1527-2024, 2024.
 - Ziemann, P. J. and Atkinson, R.: Kinetics, products, and mechanisms of secondary organic aerosol formation, Chem. Soc. Rev., 41, 6582–6605, https://doi.org/10.1039/c2cs35122f, 2012.